

Using DC resistivity method to characterize the geometry and the salinity of the Plioquaternary consolidated coastal aquifer of the Mamora plain, Morocco

B. Benkabbour · E.A. Toto · Y. Fakir

Abstract The Direct Current resistivity method was applied to the consolidated coastal Plioquaternary aquifer of Mamora plain, located on the Atlantic coast of Morocco. The aim is to determine the depth of the base of the saturated zone in the aquifer and to help in imaging lateral and vertical distribution of groundwater salinity. The geoelectric survey showed four geoelectric formations with the following electrical resistivities from top to bottom: 20–80, 200–2000, 200–300 and 5–70 Ohm m. The latter designates the basement of the aquifer constituted of marls and sandy marls. The mean resistivity of 250 Ohm m designates the aquifer formation. It decreases to less than 25% of its initial values for the soundings near the shore, reflecting the oceanic impact on the aquifer formation resistivity. The contour map shows that the basement of the saturated zone in the aquifer is deeper in the Northwest near the Sebou River estuary with values up to 70 m below sea level. This results in a larger thickness of the saturated zone of the aquifer leading to a consequent hydraulic potential. On the other hand, it has been deduced that the extent of marine intrusion inside the continent can be governed by human activities, natural properties and substratum

geometry of the aquifer as well as by ecological factors. An optimal network of electrical soundings has been proposed for the monitoring of saltwater intrusion.

Keywords Seawater intrusion · Plioquaternary aquifer · DC resistivity · Mamora plain · Morocco

Introduction

The Mamora coastal plain is located in the northwest of Morocco on the Atlantic littoral coastal region (Fig. 1). This region has an area of about 390 km², 50% of which is covered by one of the most important cork oak forests in the world.

It has a Mediterranean climate with temperatures varying from 13 °C in winter to 27 °C in summer. The mean annual precipitation is about 500 mm·year⁻¹. The Sebou River (3 billion m³·year⁻¹) crosses the region in the north. Ocean tide effects on the river were felt up to tens of kilometers away from the shore (Combe 1975).

Escalating stresses due to anthropogenic activities are affecting the Plioquaternary aquifer, formed by calcarenitic and sandstone rocks. Indeed, the socio-economic development of the area is generally dependent on groundwater pumping. Parallel growth of population, agriculture and industry has occurred especially near the Atlantic Ocean shore and the Sebou River estuary. The Kenitra Province, involving the study area, has 1 million inhabitants; 56% of which live in rural areas. Agriculture is the principal activity in the region and 53% of industries are involved the agri-food sector (DRPE 1989). Pumping discharge is 38 million m³·year⁻¹ used with a proportion of 75% for drinking and industrial needs and 25% for agriculture (DRPE 1989). Kenitra city is supplied by three municipal pumping stations (Fig. 2).

Though many pumping wells were abandoned because of high salinity during previous accentuated dry periods, presently the groundwater salinity remains moderate at a

Received: 18 February 2002 / Accepted: 23 August 2003
Published online: 15 October 2003
© Springer-Verlag 2003

B. Benkabbour
Department of Geology, Faculty of Sciences and Techniques,
P.O. Box 597 Beni Mellal, Morocco

E.A. Toto
Department of Geology, Faculty of Sciences,
University Ibn Tofail, P.O. Box 133 Kenitra, Morocco

Y. Fakir (✉)
Department of Geology, Faculty of Sciences,
P.O. Box 2390 Semailia, Marrakech, Morocco
E-mail: fakir@ucam.ac.ma
Tel.: +212-44-434649
Fax: +212-44-437411

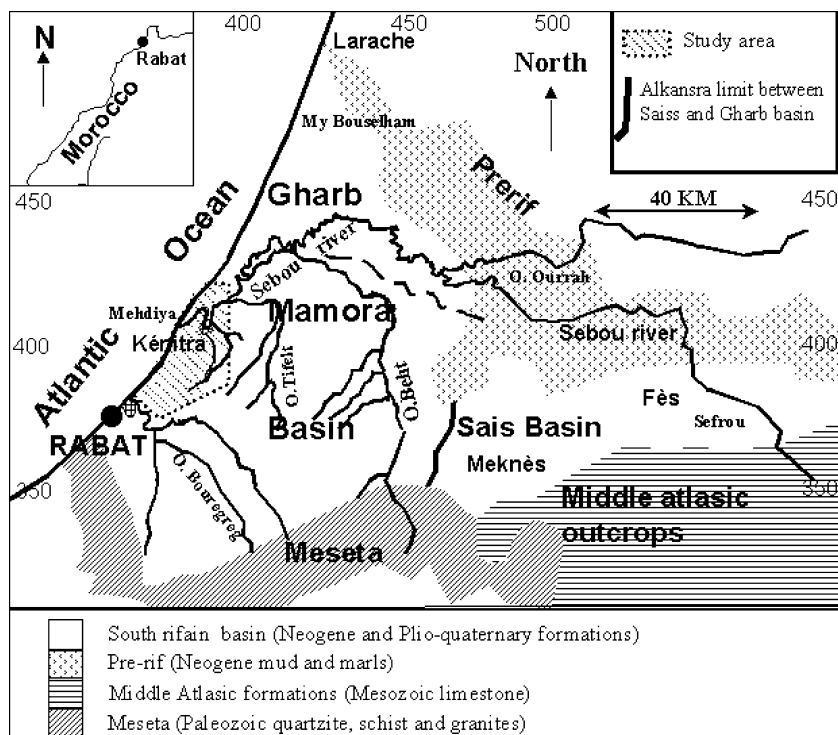


Fig. 1
Situation of the studied area and its local geology

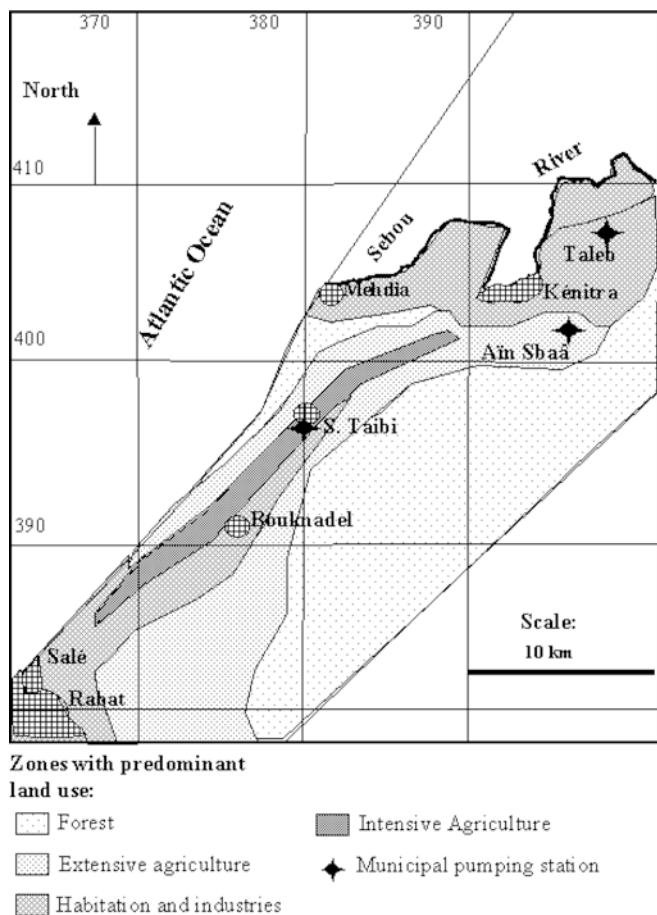


Fig. 2
Coastal Mamora land use map as deduced from topographic maps, aerial photography and field missions

regional scale. However, an increase of groundwater salinity towards the ocean and over tens of kilometers along the Sebou River estuary is observed (Fig. 3, Table 1). In this study, the Direct Current resistivity method is used to measure the electrical properties of the coastal aquifer system of Mamora. This method, which in recent years has undergone a resurgence in interest due to advances in data acquisition technology, better mathematical algorithms and more interactive modeling software (Merrick 1997), has given good results in exploring groundwater productivity (Bose and Ramakrishna 1978), salinity and saltwater intrusion (Fretwell and Stewart 1981), geothermal properties (Thanassoulas and others 1986) and anthropogenic pollution (Adepelumi and others 2001, Kundu and others 2002). The DC resistivity method can be used successfully in a variety of different sedimentary and non sedimentary rocks. However, some difficulties can arise in clay rich or faulted formations. Those difficulties may be obviated by combining this method with others such as the electromagnetic (Arora and Bose 1981) or induced polarization (Seara and Granda 1987) methods. In the present study, the DC resistivity method is applied to explore the water table aquifer in the Plioquaternary, faulted, consolidated sandstone with no clay content in the saturated zone. In areas with faults, a technique inspired from offset Wenner profiling (Hobbs and Reading 1987) is used. Hence, the main objective of the research is to determine the geological structure, the depth of the marly base of this aquifer and to assess groundwater salinity distribution in both lateral and vertical directions.

Correlation between geoelectrical, hydrogeological and land use data, allow us to determine factors involved in groundwater vulnerability to marine intrusion and to

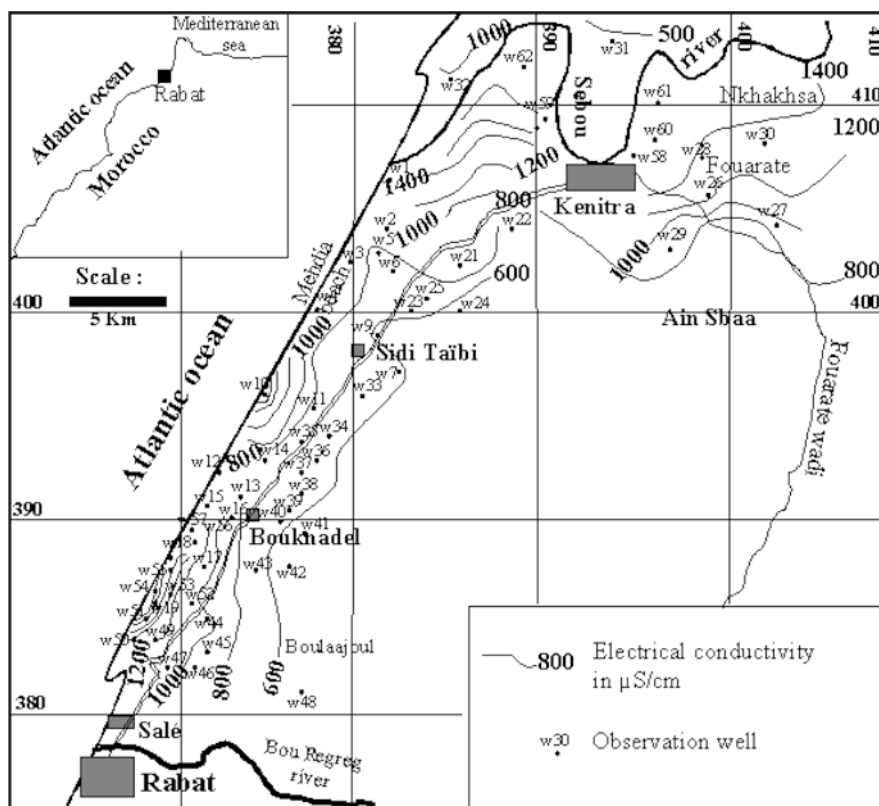


Fig. 3
Areal distribution of electrical conductivity (July 2000)

Table 1
Observation wells and the relevant electrical conductivity (July 2000)

Wells	Lambert coordinates		Z (m)	Electrical conductivity ($\mu\text{S}/\text{cm}$)	Wells	Lambert coordinates		Z (m)	Electrical conductivity ($\mu\text{S}/\text{cm}$)
	x (km)	y (km)				x (km)	y (km)		
w1	381,000	402,250	06	1,438	w32	384,800	409,150	06	1,069
w2	380,550	401,600	08	0920	w33	381,300	396,550	40	0680
w3	380,300	401,100	08	1,246	w34	397,700	396,450	15	0679
w4	379,750	400,300	10	1,160	w35	379,450	396,550	06	0636
w5	381,900	402,000	50	0587	w36	380,500	394,800	37	0677
w6	382,000	401,400	20	0533	w37	380,400	394,400	45	0720
w7	382,250	398,350	35	0632	w38	379,800	394,300	48	0701
w8	383,000	404,000	37	0654	w39	378,650	393,300	65	0636
w9	380,630	399,850	08	0587	w40	378,100	393,200	52	0647
w10	378,900	398,200	10	2,521	w41	377,200	392,350	45	0521
w11	379,000	397,550	08	0570	w42	376,650	391,250	45	0543
w12	376,700	395,200	20	0969	w43	376,350	390,700	39	0770
w13	376,300	393,550	28	0781	w44	375,650	388,750	45	1,047
w14	376,750	394,250	27	0570	w45	373,800	388,100	45	0930
w15	373,150	389,800	21	2,170	w46	373,150	387,600	45	0867
w16	373,000	389,900	46	0953	w47	372,700	386,800	45	1,192
w17	372,100	388,500	15	1,133	w48	372,200	382,300	70	0596
w18	372,200	388,600	32	1,739	w49	369,850	385,250	17	1,240
w19	370,600	386,400	20	1,512	w50	365,500	385,450	22	1,271
w20	369,750	385,800	30	1,631	w51	369,900	385,500	20	1,481
w21	388,350	406,800	07	0973	w52	370,500	386,000	22	1,019
w22	388,600	408,750	40	0647	w53	371,600	387,800	22	1,322
w23	382,750	401,550	10	0773	w54	371,400	388,000	35	2,470
w24	383,330	402,500	15	0572	w55	372,500	389,100	35	0521
w25	383,080	402,760	25	0625	w56	372,800	389,500	42	1,736
w26	395,100	408,900	03	1,260	w57	389,400	373,000	20	2,631
w27	396,900	409,100	10	0965	w58	392,850	409,000	07	2,800
w28	396,600	411,500	08	1,376	w59	390,150	408,600	05	1,800
w29	396,800	413,100	04	0906	w60	392,580	409,440	03	4,300
w30	397,000	413,200	05	1,304	w61	392,970	410,230	05	3,000
w31	392,100	412,500	07	0557	w62	389,700	411,150	10	0700

establish an optimal network of electrical soundings for monitoring this saline contamination.

Geohydrology of coastal Mamora

The coastal part of Mamora plain is limited to the south by the Meseta, which is a Paleozoic tabular and stable bedrock (Flinch 1993), and to the north by the Rharb plain, which is a recent, and subsiding basin belonging to the Rifan domain (Fig. 1). The Paleozoic bedrock is covered by Miocene blue marls, Pliocene calcarenites, then by Quaternary sandstones and sands.

The Mamora coastal plain has a phreatic, consolidated and faulted aquifer. Its substratum is constituted by Miocene blue marl. Its saturated and unsaturated zones are generally made of calcarenitic and sandstone rocks, with high transmissivities (up to $1.5 \cdot 10^{-01} \text{ m}^2 \cdot \text{s}^{-1}$). The as yet unpublished modeling of Mamora groundwater flow shows that values for hydraulic conductivity and effective porosity range respectively from $1.2\text{E}-04 \text{ m/s}$ up to $2.25\text{E}-03 \text{ m/s}$ and between 3 and 15%. The aquifer may involve different types of flow circulation. Indeed, it has been found that groundwater velocities around the Sidi Taibi pumping station fluctuate as follows (ONEP 1995):

- from 125 to 342 m/day^{-1} , attributed to flow through karstic channels;
- from 34 to 75 m/day^{-1} , attributed to flow through fissures;
- from 9 to 17.5 m/day^{-1} , attributed to flow through interstitial porosity.

These measurements were performed by following the aquifer geoelectrical properties after tracing groundwater with salt injections inside a selected network of wells. Two hydraulic units may be distinguished (Fig. 4). The northern unit of Sebou where the flow seems to be controlled by the river level and where hydraulic gradients are very low. This unit is separated from the southern one by the hydraulic divide of Sidi Taibi. Within the latter, groundwater flows generally northwestwards to the Atlantic ocean following higher hydraulic gradients. Salinization processes are occurring nearby the coastline and the Sebou River estuary (Fig. 3). Within the affected areas, the groundwater chemical facies changes from a calcium bicarbonate type to a sodium chloride type (Ben Kabbour 2002) and therefore the hydraulic potential is gradually decreasing. Because of the pumping activities and the ocean boundary, the salinization seems to be mainly related to the effects of a seawater intrusion.

Materials and methods

Most geological materials are composed of electrically insulating minerals. Rocks can then conduct electricity through water filled pores and fractures. It has been found that electrical resistivity of a formation is proportional to the electrical resistivity of the saturating pore fluid and inversely proportional to the porosity raised to a power (Archie 1942). More precisely the following relationship was developed:

$$F = \rho_f / \rho_w = a \cdot \phi^{-m}$$

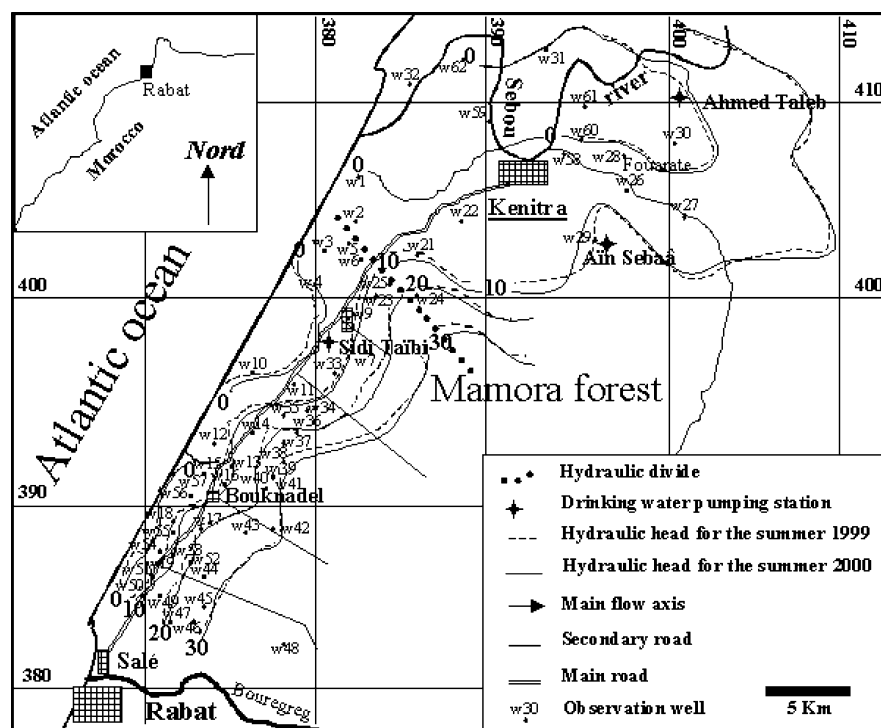


Fig. 4
Piezometric map of the coastal aquifer of Mamora (July 2000)

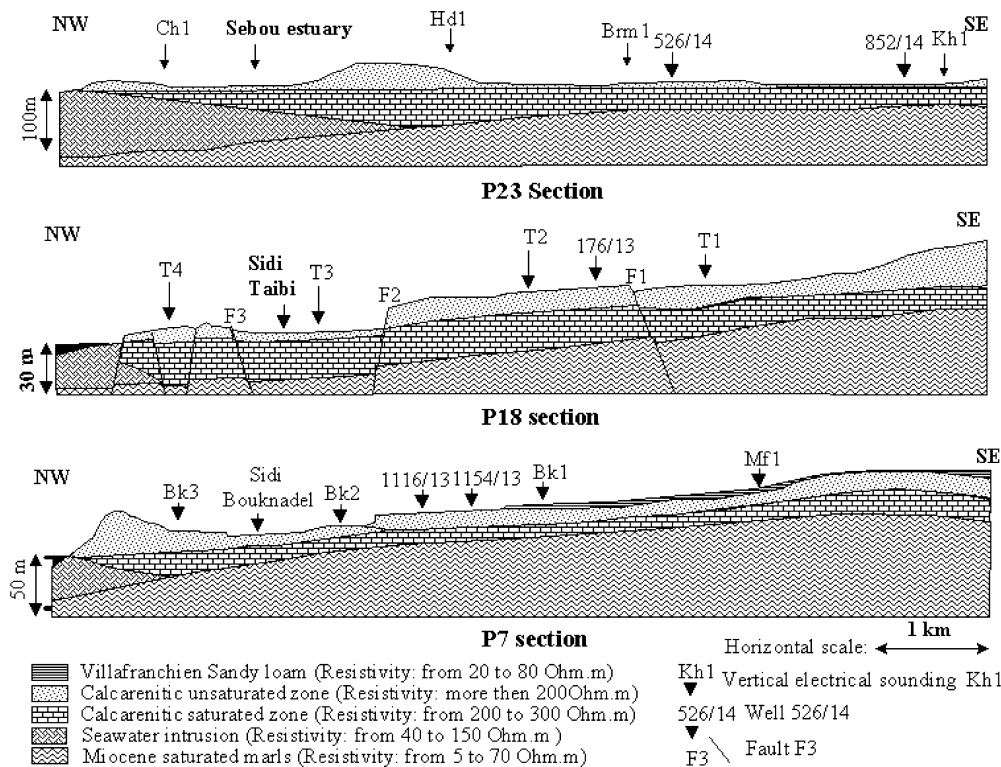


Fig. 5 NW-SE geological sections as deduced from electrical resistivity profiles and well logs (see location in Fig. 9)

where F is the formation factor, ρ_f is the formation resistivity, ρ_w is the pore fluid resistivity, ϕ is the porosity, a is the tortuosity and m the cementation factor; the two latter factors are specific to a formation. There are several factors which can influence the resistivity given by Archie's law. First Archie's law does not include the internal surface conductivity (clay content) and the presence of clay minerals in the pore space reduces the formation resistivity by their cation exchange capacity. This phenomenon is well pronounced for geological formations with a resistivity of less than 10 ohm m (Keller and Frischknecht 1966). Consequently, the clay layers make it difficult to discriminate between regions of the aquifer with marine intrusion and regions of clays, which had equally low resistivities; a combination of the DC resistivity method with the induced polarization method can give good results in areas with intercalations of clay-rich formations (Seara and Granda 1987). Second, the presence of faults and fractures in an aquifer can have two different impacts; if the fractures and faults are opened and filled with water they lower the predicted formation resistivity but if those fractures and faults are filled with insulator materials they can obstruct the passage of electrical current and then increase the formation electrical resistivity. In the DC resistivity method a Direct Current is driven through the ground using four-terminal electrodes. The Schlumberger array was used in our example to study variations in resistivity with depth through vertical soundings. Current is driven through one pair of electrodes; the potential established in the earth by this current is measured with the second pair of electrodes. Using the current intensity and the generated potential, the apparent resistivity of the earth can be measured by using

Ohm's Law and the geometric characteristics of the spacing between the various electrodes (Griffiths and King 1965; Keller and Frischknecht 1966; Seguin 1985; Stadelhofen and Meyer 1991). The resistivimeter GEOTRADE (Geotrade 2000) and the computer program GRIVEL (BRGM 1988) are then used respectively for the acquisition and the compilation of the geoelectrical data. The survey, which covers about 390 km² at a line and current electrodes spacing varying from 300 to 1000 m, counts more than 60 Vertical Electric Soundings (V.E.S.) located in a 5 km wide zone parallel to the ocean. We began by exploring the electrical properties of the geological formations by sounding directly on the outcrops and near wells with geological and geophysical logs.

Results and discussion

Vertical variation of the aquifer formation resistivity

The amount of data recorded provides an insight into the three-dimensional distribution of geoelectric parameters in the area. The resistivity is deduced from laboratory measurements of both the aquifer formation porosity and water resistivity.

The interpretation of the apparent resistivity curves was performed in two stages. During the first stage we used two and three layer model curves (Astier 1971) and with the auxiliary point method we determined an approximate geoelectric model. Next, we used the Grivel computer program to improve the above model until the RMS difference between observed and calculated data was less

than 5%. The geoelectric model thus reflects a possible geoelectric section. The interpretation of the resistivity is shown for the traverses P7, P18 and P23 located respectively near the sites of Sidi Bouknadel, Sidi Taibi and Sebou River. As seen from those profiles, the following formations can be identified (Fig. 5):

1. Surface formations covering the investigated area present large lateral variations in their electrical resistivity and thickness. For surface sandy loam at the east of the profile P7, the mean resistivity varies from 20 to 80 Ohm m.
2. The next geological formation is almost uniform on all traverses, it was identified as sand and calcarenitic formations, with electrical resistivity values lying between 200 and 2000 Ohm m depending upon the relative amount of concentrated sand, gravels and conglomerates and depending upon the existence of faults and karsts.
3. The aquifer formation is identified with a mean resistivity of 250 Ohm m. This resistivity is lowest in the west of all the profiles and decreases too less than 25% of its initial values for the soundings near the sea. This decrease reflects the seawater intrusion impact on the aquifer formation resistivity.
4. The last and deepest formation has a very low electrical resistivity generally between 5 and 70 Ohm m. This formation is constituted of the marls and sandy marls of the aquifer bottom.

Spatial variation of the aquifer substratum geometry

The spatial variation of the aquifer substratum altitude for the whole of the investigated area (Fig. 6) shows that the

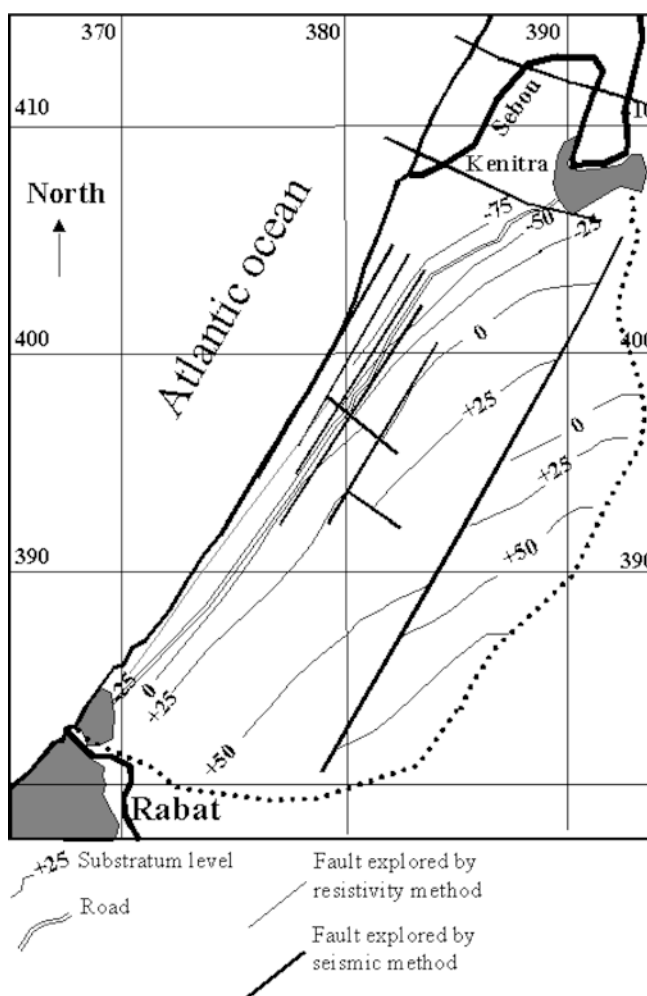


Fig. 6
Structural map of Mamora coastal aquifer substratum

Fig. 7

Some vertical electrical soundings showing the impact of water salinity on the aquifer electrical resistivity

G1 sounding model

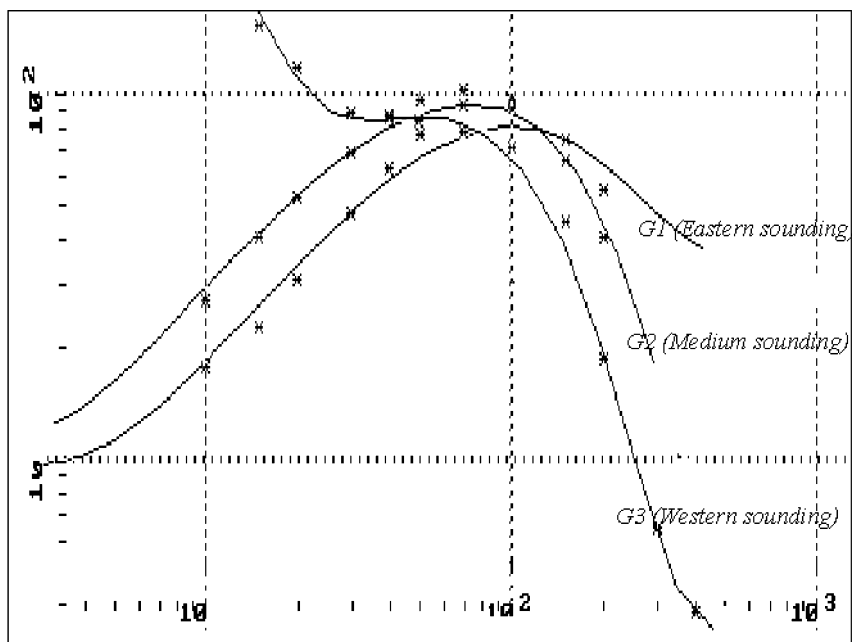
n	Thickness	Depth	Resistivity
1	4.9	0.	8.9
2	4.9	4.9	1136
3	7.3	9.8	203
4	11	17	76
5	∞	28	27

G2 sounding model

n	Thickness	Depth	Resistivity
1	3.22	0.	10.15
2	2.47	3.22	670.05
3	5.07	5.69	377.13
4	39.35	10.76	91.68
5	17.85	50.11	90.70
6	∞	67.96	1.89

G3 sounding model

n	Thickness	Depth	Resistivity
1	8	0.	370
2	9.4	8	30
3	25	17	169
4	9.2	42	50
5	∞	51	1.5



zone with the deeper substratum is downstream of Sebou River where the substratum level is situated at more than 70 m below sea level. This results in a large thickness of aquifer saturated zone leading to a consequent hydraulic potential.

Many faults are detected upstream in the recharge area under the Mamora forest using a technique inspired from offset Wenner profiling (Hobbs and Reading 1987). Those faults have a direction parallel to the coast and can coincide with highly productive zones in the aquifer (Zouhri and others 2001).

Groundwater salinity distribution

The resistivity values are highly influenced by the proximity of the ocean. For example, from a distance of 200 m spacing between the current electrodes, the lowest resistivity is observed in the G3 soundings, which are 500 m from the sea, and the highest resistivity is observed in the G1 sounding, which is 2000 m from the sea (Fig. 7). The lower resistivity at the beginning of the eastern sounding is caused by a 5-m thick clay-rich layer on the surface separated from the aquifer by a 5-m thick high resistive unsaturated zone. Hence, the aquifer remains unconfined in this part of the studied area in spite of the existence of the surface clay-rich formation. The aquifer formation resistivity decreases too less than 50 Ohm m northeast and southwest of the region (Fig. 8), in areas where salinization processes are observed. If we relate this lowest resistivity to the sole impact of seawater intrusion, the coastal area downstream of Sidi Bouknadel and downstream of Sebou River are the most affected by seawater contamination (Fig. 8). The area of Sidi Taibi is also affected, but to a lesser extent. Vertically, the seawater wedge seems to penetrate 3 km inside the continent for the profile P23, 1 km for the profile P7 and is of a local extent for the profile P18 (Fig. 5).

Seawater intrusion factors and geophysical monitoring

In addition to pumping activities, several factors may explain the variable extent of seawater intrusion from sector to sector.

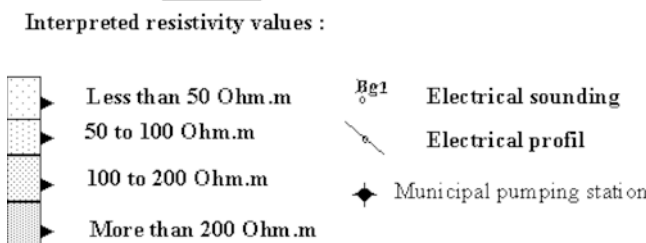
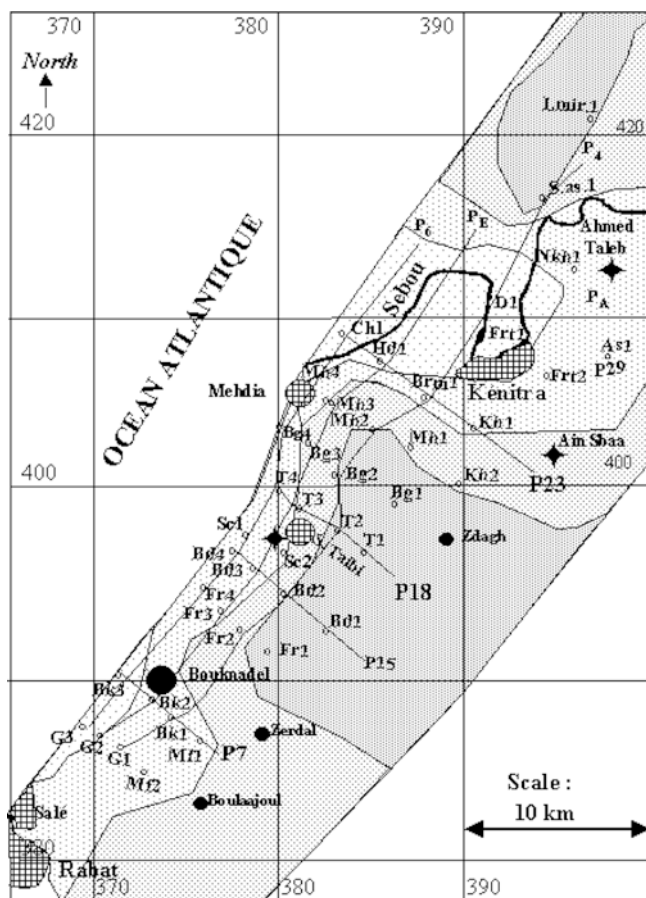


Fig. 8
Interpreted resistivity of the Mamora coastal aquifer

One of the several equations deduced from the Ghyben-Herzberg equation, describing the geometry of the fresh-saline interface in relation to the hydrogeologic characteristics of the aquifer and rates of fresh

Table 2
Optimal network of electrical soundings for monitoring salt-water intrusion

Area	Electrical sounding	X	Y	Z	Bottom elevation (m)
Sidi Bouknadel	G1	373.100	388.800	20	-8
	G2	372.700	389.100	10	-25
	G3	371.250	387.200	10	-25
Sidi Taibi	Fr4	376.800	395.000	15	-18
	SC1	379.300	397.000	10	-25
	SC2	381.200	396.700	20	-10
South of Kenitra City	HD1	385.800	408.800	25	-100
	Brm1	387.400	405.500	10	-45
	Kh1	391.400	404.500	10	-22
Ahmed Taleb	D1	392.000	411.200	2	-50
	Nkh1	396.800	412.200	3	-35

groundwater flow (Todd 1980; Domenico and Schwartz 1990), is as follows:

$$L = \frac{\rho_f}{\rho_s - \rho_f} \times \frac{K \cdot m^2}{Q}$$

where ρ_f is the density of freshwater and ρ_s is the density of seawater.

It shows that the landward extent of the saline water wedge (L) is directly proportional to the hydraulic conductivity (K) and the square of the aquifer thickness (m), and inversely proportional to the flow of freshwater to the sea. Consequently, in the area of Sebou River, the wide extent of seawater intrusion can be explained by the high depth of the aquifer substratum leading to the large thickness of the aquifer. High permeability could also be invoked because of the very low hydraulic gradients and the probable existence of fault directions perpendicular to the coast (Zouhri and others 2001).

On the other hand, ecological factors also make an important contribution. The Sebou River constitutes, indeed, a pathway for seawater into the mainland. Therefore, seawater contamination may occur directly from the ocean near the coastline as well as via the Sebou riverbed several tens of kilometers inland. Concerning the Sidi Taibi sector, the forest near the coastline (Fig. 2) is preserved by law, leading to a lower intensity of exploitation of groundwater for irrigation use and thus to less seawater intrusion.

Traditional shallow wells with small withdrawals as well as the probable karstic flow circulations would contribute to keeping groundwater salinity at generally acceptable levels. An optimal network of electrical soundings (Table 2) can be chosen from all the soundings to monitor saltwater intrusion. We can use for the site of Sidi Bouknadel soundings G1, G2, G3; for the site of Sidi Taibi soundings Fr4, Sc1, Sc2; for the area closer to Kenitra city soundings Hd1, Brm1, Kh1 and finally soundings D1, NKh1 for the area of Ahmed Taleb (Fig. 8). These soundings are easy to access, located in areas where the aquifer basement is under the sea level and downstream of municipal pumping stations.

Conclusions

The DC resistivity method works very well in the Mamora coastal aquifer even if the aquifer is consolidated and covered by very resistant surface soils.

Many geoelectric documents were produced. It has been shown that the zone with the deeper substratum is downstream of Sebou River, resulting in a large thickness of the saturated zone of the aquifer and then a consequent hydraulic potential. This thickness may, on the other hand, be an important factor leading to the wide extent of seawater wedge in this sector. This is, indeed, a significant example, which shows that in coastal areas, the productive zones are often the most vulnerable to seawater intrusions. Ecological factors, such as the presence of the forest cover and the Sebou Estuary, are also controlling

seawater intrusion. Therefore groundwater resources management should take into account all the Mamora ecosystem compounds for water development planning as well as for protection measures against groundwater salinization.

References

- Adepelumi A, Ako B, Ajayi T (2001) Groundwater contamination in the basement-complex area of Ile-Ife, southwestern Nigeria: a case study using the electrical-resistivity geophysical method. *Hydrogeology J* 9:611–622
- Archie GE (1942) Electrical resistivity as an aid in core analysis interpretation. *T Am I Min Eng* 146:54–62
- Arora CL, Bose RN (1981) Demarcation of fresh- and saline water zones, using electrical methods (Abohar area, Ferozepur district, Punjab). *J Hydrology* 49(1/2):75–86
- Astier JL (1971) *Géophysique appliquée à l'hydrogéologie*, Masson et Cie, Paris
- Ben Kabbour B (2002) *Exploration, évaluation et protection des eaux souterraines de la Mamora côtière (Maroc): approches géophysique, hydrogéochimique, modélisation et S.I.G.* PhD Thesis, Faculté des Sciences Kénitra, Maroc, 280 pp
- Bose RN, Ramakrishna TS (1978) Electrical-resistivity surveys for groundwater in the Deccan trap country of Sangli District, Maharashtra. *J Hydrology* 38(3/4):209–221
- BRGM (1988) *Manuel d'utilisation de Grivel*. Orléans, France, 20 pp
- Combe M (1975) Le bassin Gharb-Mamora et les petits bassins septentrionaux des oueds Dradere et Soueire. In: *Notes & Mémoires du Serv. Géol. Maroc* 231(2):93–128
- Domenico PA, Schwartz FW (1990) *Physical and chemical hydrogeology*. Wiley, New York, 824 pp
- DRPE (1989) *Etude du plan directeur intégré d'aménagement des eaux des bassins de Sebou, Bouregreg, Oum Er rbia et Tensift. Ressources en eaux souterraines. Note de synthèse*, 20 pp
- Flinch JF (1993) *Tectonic evolution of the Gibraltar Arc*. PhD Thesis, Rice University, Houston, 381 pp
- Fretwell JD, Stewart MT (1981) Resistivity study of a coastal karst terrain, Florida. *Groundwater* 19(2): 156–162
- Geotrade (2000) *Manuel d'utilisation du résistivimètre*. Geotrade, Switzerland
- Griffiths DH, King RF (1965) *Applied geophysics for geologists and engineers. The elements of geophysical prospecting*. Pergamon Press, Oxford, 230 pp
- Hobbs BA, Reading AM (1987) Shallow faults location in coal measures using offset Wenner resistivity profiling. *Geophys Prospect* 42:343–356
- Keller YGV, Frischknecht FC (1966) *Electrical methods in geophysical prospecting*. In: *International series in electromagnetic waves*, vol 10. Pergamon Press, Oxford, 519 pp
- Kundu N, Panigrahi MK, Sharma SP, Tripathy S (2002) Delineation of fluoride contaminated groundwater around a hot spring in Nayagarh, Orissa, India, using geochemical and resistivity studies. *Environ Geol* 43:228–235
- Merrick NP (1997) The electrical resistivity method. In: Zannetti P (ed) *Environmental modeling volume 3: computer methods and software for simulating environmental pollution and its adverse effects*. Computational Mechanics Publications, Southampton, Boston, 496pp
- ONEP (Office National de l'Eau Potable) (1995) *Etude de traçage au sel dans le champs captant de sidi Taibi. Suivi du traçage par prospection électrique*. ONEP/GTZ, Maroc
- Seara JL, Granda A (1987) Interpretation of IP time domain/resistivity soundings for delineating sea-water intrusions in

- some coastal area of the Northeast of Spain. *Geoexploration* 24:153–167
- Seguin Mk (1985) *La géophysique et les propriétés physiques des roches*. Les presses de l'Univ Laval, Québec
- Stadelhofen MK, Meyer C (1991) *Applications de la géophysique au recherches d'eau*. Techniques et documentation, Lavoisier, France
- Thanassoulas C, Tselentis G-A, Kolios N(1986) Geothermal prospecting by geoelectric soundings in NE Greece. *Geophysical Prospecting* 34:83–97
- Todd DK (1980) *Groundwater hydrology*. Wiley, New York
- Zouhri L, Lamouroux C, Vachard D, Pique A (2001) Les corps perméables plio-quaternaires de la Mamora (Maroc). *Géométrie et influence structurale*. *Earth Planet Sci* 332:1–4